2022 IEEE PES Innovative Smart Grid Technologies Conference Europe (ISGT-Europe) | 978-1-6654-8032-1/22/$31.00 ©2022 IEEE | DOI: 10.1109/ISGT-Europe54678.2022.9960485

Impact of distributed energy resources on power system resilience against earthquakes

Jihad Guenaou
BEAMS - Electrical Energy
Université Libre de Bruxelles
Brussels, Belgium
jguenaou@ulb.be

Pierre Henneaux
BEAMS - Electrical Energy
Université Libre de Bruxelles
Brussels, Belgium
pierre.henneaux@ulb.be

Daniel S. Kirschen
Dept. of Electrical and Computer Engineering
University of Washington
Seattle, WA, USA
kirschen@uw.edu

***Abstract*—Distributed energy resources (DERs) can enhance power system resilience against natural disasters. However, a high penetration of DERs changes the structure and dynamics of power systems at the transmission level. Their overall impact on resilience requires a thorough analysis. This paper describes a probabilistic resilience assessment method to assess how different levels of DERs penetration affect the system dynamics at the transmission level. Using a modified version of the IEEE-39 test system, it quantifies how DERs can affect the resilience of the system to earthquakes. Additional probabilistic sensitivity studies investigate the effect of inertia on the resilience. Finally, the analysis of a specific scenario illustrates the effect of the DERs on the dynamics of the power system.**

***Index Terms*—Natural disasters, power transmission system, resilience, Monte Carlo simulations, distributed energy resources**

I. Introduction

Several groups of researchers (e.g., [1]–[3] have discussed methods to assess the resilience of power systems to natural disasters as well as techniques to enhance this resilience. Some of these assessment techniques are probabilistic methods based on Monte Carlo simulations, where sets of scenarios model the consequences of natural disasters by simulating the failure of randomly selected power system components. Resilience is then measured using probabilistic indices that reflect the behavior of the power system in response to these failures as well as the time required to restore service. These various probabilistic assessment method differ mostly in the way they model the effect of the disturbances on the power system. In [4], [5], an AC power flow provides a static model of the grid and the presence of distributed energy resources (DERs) is not discussed. On the other hand, Faghihi et al. [6], use a more realistic dynamic power system model, but also focus their study on conventional power systems. While very effective, probabilistic methods do not provide a complete picture of how power systems with a high penetration of DERs will be affected by natural disasters. The first part of this paper presents a method to model DERs in studies aimed at developing resilience enhancement strategies. The case studies in the second part of the paper assess the impact of the presence of DERs on the resilience of a transmission grid against earthquakes. The conclusions drawn from the results will allow the development of enhancement strategies adapted to power systems with high penetration of DERs.

978-1-6654-8032-1/22/$31.00 ©2022 IEEE

II. Method

The introduction of DERs increases the system sensitivity to frequency and voltage variations because they lessen the need for conventional generators and thus reduce the number of synchronous machines that contribute inertia and voltage support to the system. On the other hand, DERs supply loads more locally and thus reduce the loading on the transmission grid, which makes the power system less sensitive to lines failure. Adequately modeling these different effects requires a dynamic modeling of the power system. Section II-A describes the probabilistic resilience assessment method followed to assess the resilience. Section II-B details the dynamic model of the system.

The share of the demand supplied by DERs has a profound effect on the way the system is operated. Subsection II-C describes how realistic test cases are prepared by solving Unit Commitment (UC) and Optimal Power Flow (OPF) problems.

A. Probabilistic resilience assessment

The method is based on [6], in which a probabilistic assessment for power system resilience against extreme events has been developed. The resilience assessment is conducted in three steps: (i) the threat characterization, (ii) the system vulnerability modeling, (iii) the system reaction simulation.

1) Threat characterization: The threat is characterised in a probabilistic manner in order to capture the stochastic nature of such events. The considered characteristics of an earthquake are: its location, depth and magnitude. These are defined as stochastic variables modeled by probability density functions. This leads to the definition of a set of earthquake scenarios, that correspond to different values of the stochastic variables generated using Monte Carlo simulations [7], [8].

2) System vulnerability modeling: The system vulnerability is derived from the fragility curves of the power system

elements (i.e. transmission lines, substations and generators). For each earthquake scenario, a set of contingencies is generated based on the latter curves.

3) System reaction simulation: The system reaction is assessed by means of a dynamic approach, in order to consider the power system transients and time of failures. The power system model and the different contingencies are implemented in EUROSTAG software. It simulates the dynamics of the power system using an implicit integration method while solving the differential and algebraic equations of the system at each time step [9].

B. Power system dynamic modeling

To model the power system, 2 sub-systems are considered: the transmission network and the distribution network.

As the study focuses on transmission network dynamics, a detailed model is implemented considering the synchronous generators (SGs) and their control systems, transmission lines, transformers and protection systems. Regarding the distribution network, equivalent models are derived considering loads and DERs dynamics. Indeed, a trade off between the complexity (i.e. high computation time) and the accuracy is necessary at this stage. However the complexity of the models for loads and DERs can always be improved and adapted for more specific studies (e.g. enhancement strategies studies).

1) Load dynamics: Loads are considered at the transmission network level. Each bus can hold a maximum of on load. Each load dynamic is governed by the following equations [10]:

$$P_L(t) = (P_L(t_0) + A_p(t - tp))(\frac{|U|}{|U_{filtre}|})^2(\frac{f}{f_0})^\gamma \quad (1a)$$

$$Q_L(t) = (Q_L(t_0) + A_q(t - tq))(\frac{|U|}{|U_{filtre}|})^2(\frac{f}{f_0})^\delta \quad (1b)$$

$$\frac{dU_{filtre}}{dt} + \frac{1}{T}U_{filtre} = \frac{1}{T}U,\ U_{min} < U_{filtre} < U_{max} \quad (1c)$$

Where $P_L(t)$ and $Q_L(t)$ are respectively the active power and reactive power consumed by the load at time t, $P_L(t_0)$ and $Q_L(t_0)$ are respectively the initial active power and reactive power consumed by the load a derived for the AC PSOPF, A_p in MW/s and A_q in MVar/s are the variation in function of time imposed to the load, t_p and t_q the last times before t at which variations were imposed, U is the voltage at time t of the node to which the load is connected, f and f_0 are respectively the frequency at time t and time t_0 of the power system, γ and δ are coefficients defined for each load that specify its dynamic and T the time constant of the transformer tap change.

EUROSTAG allows easy implementation of such load dynamic thanks to predefined modules.

2) DERs dynamics: Different techniques exist to develop dynamic models of DERs. These can be divided into two categories, reduction techniques and parameter identification techniques [11], [12].

The techniques of the first category are based on the set of differential-algebraic equations defining the system dynamics. Their main objective is to simplify the set of equations by reducing the system model order. The most used technique is the modal approach [13], [14]. It can be defined in different steps:

- Linearization of the set of equation around a steady-state operation point.
- Deriving different modes thanks to the eigenvalues of the linearized equations.
- Considering only the mode that have an effect on the system for the dynamic study.

The techniques of the second category derive equivalent models with the same response than the system model. Data sets (measured or obtained for a simulation of the complete model of the system) are used to find the equations and to tune the parameters of the equivalents.

The methods of the first category are less suitable for extreme events than the ones of the second category as the equivalent models are only valid around a specific operational point.

The DERs dynamic model in this work is based on the model presented in the work of G. Chaspierre [11] which is developed thanks to identification techniques. It models DERs as inverter-based generators (IBGs) that are current injectors, each of them connected to a load node at the transmission level:

- The produced power P_{ref}, the measured node voltage V_m and the power system frequency f_m are the inputs of the model.
- Only the dynamic of the inverter and of its control system is considered.
- The output is the active and reactive currents I_P and I_Q injected by the IBG.

The block diagram of the IBG model implemented in this work is represented in Figure 1.

C. Preparation of base cases

As stated above, the base cases corresponding to the various PV penetration levels must reflect the way power systems are operated. Two main aspects should be considered: (i) generators not needed to economically supply the load will not be committed, and (ii) transmission systems are usually operated based on the N-1 security rule. The N-1 security rule can be enforced through a preventive and/or a corrective approach. In keeping with the most common industry practice, we will consider only a preventive approach, such that, after any contingency the state of the system has to respect all operating constraints without requiring operator intervention [15]. A Preventive Security-Constrained OPF (PSCOPF) considering UC constraints can thus be adopted. As these base cases will be used afterwards in dynamic simulation, the full AC power

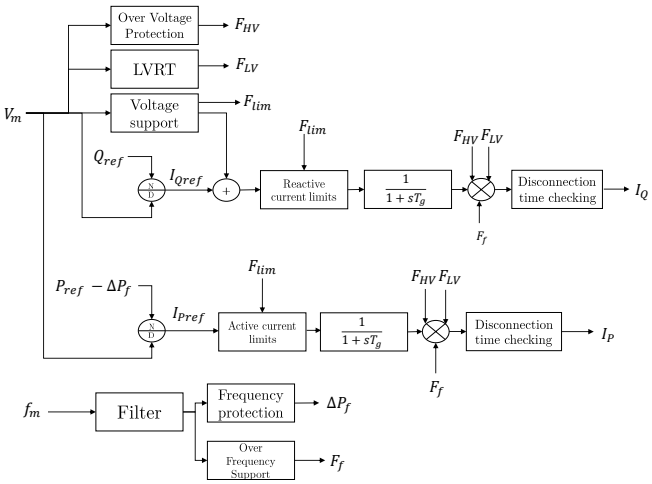

Fig. 1. Block diagram of the IBG model

flow equations must be used. However, integrating binary variables describing the commitment status of generating unit in a AC PSCOPF results in a Mixed Integer Non-Linear (MINLP) optimization problem. Because the problems of this class are notoriously difficult to solve, we decouple this problem into: (i) a Mixed Integer Problem (MIP) to find the commitment status of generating units through a DC PSCOPF considering UC constraints, and (ii) a Non-Linear Programming (NLP) problem to find the optimal generation pattern and voltage setpoints for the UC solution obtained using the MIP problem through a AC PSCOPF. This decomposition is similar to the one adopted in [16], except that lines are not considered as switchable here.

III. Case study

A. Test system

The methodology described previously is applied in this section on an adapted and enhanced version of the IEEE 39-bus system, often called the 39-bus, 10-machine New England System. Dynamic data for classical generators (synchronous machines, excitation systems and turbine-governor systems) are the ones corresponding to the modified IEEE 39-Bus Modified Test System proposed by [17]. A major modification relates to generator 10 (bus 39). As it is supposed to be the aggregation of a large number of generators (i.e., the rest of the Eastern Interconnection), a large inertia is associated to it in the original version. However, in the modified version, a small inertia is used. In order to consider properly cascading effects, the following protection systems are considered: under- and overvoltage relays and under- and over frequency relays for the generators, power overload relays for transmission lines, as well as a multi-level underfrequency load shedding scheme. The IEEE 39-bus system has 19 loads totaling 6097.1 MW and 1408.9 MVAr. These values are considered to be the peak loads. As the maximum PV generation is usually not reached during the peak, the load level considered in this work is 90% of the peak. The restorative load modelled described in II-B is used with a time constant of 5 seconds. Techno-economic data of generating units are taken from the IEEE PES Power Grid Library [18], with a technical minimum considered to be 50% of the nominal capacity.

Regarding the earthquake scenarios, the impact on substations, leading to the loss of transmission lines, is considered. All the substations have the same fragility curve. The potential loss of generators and DERs is ignored as the main objective is to explore different level of DERs penetration.

B. Results

Different analyses have been conducted to explore several aspects of DERs integration. In Section III-B1, Monte Carlo simulations, with the same set of scenarios, are applied to different cases defined by their level of DERs penetration. In Section III-B2,the Monte Carlo simulations are applied to cases that differentiate by their level of inertia but have the same DERs penetration and generation.

From an initial set of 100 000 scenarios, only 1726 scenarios are kept for the Monte Carlo simulations. They correspond at minimum to N-2 events as the cases are N-1 secure. The output of each dynamic simulation i.e. an extreme event scenario, corresponds to the post-disaster steady state of the considered power system i.e. considered case. From the different outputs, average Load shedding (LS), and LS probability for different relative LS are computed.

Finally in section III-B3, the dynamic behaviour of the power systems corresponding to the different cases of Section II-C is analysed for a specific scenario.

1) DERs penetration sensitivity analysis:

Table I shows the different cases differentiated by their level of inertia and the share of DERs generation. Case 1 corresponds to the base test system without DERs (100% I with I corresponding to the total inertia of the base test system). For the 4 other cases, generators are disconnected to decrease the level of inertia and DERs generation increases.

TABLE I
Base cases

	Case 1	Case 2	Case 3	Case 4	Case 5
System inertia	100 % I	89.9 % I	79.8 % I	69.8 % I	59.5 % I
% of DERs generation	0	10	20	40	50

Figure 2 shows the curves representing the LS probability in function of the relative LS for the different cases. Case 3 is the less resilient case as it has almost the highest probability for different relative LS. It is confirmed by the results in Table II with the highest average LS and number of blackouts for Case 3. Case 1, with no DERs penetration

and Case 5 with the highest DERs penetration are the most resilient cases. The generation for the latter is more local than the other cases and it counters the negative effect of a smaller system inertia. Thus, an optimum can be found between the level of inertia and the level of local generation by DERs to maximise the resilience.

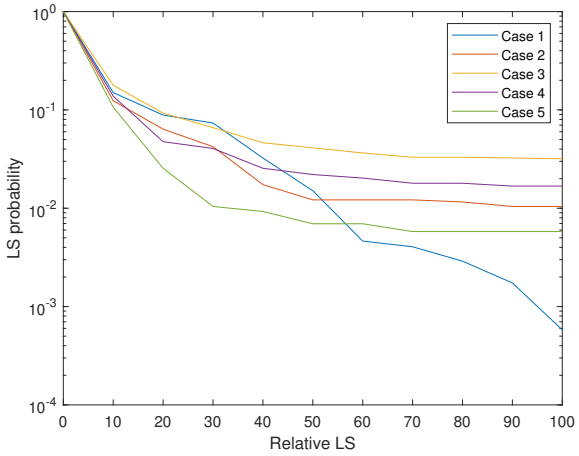

Fig. 2. LS probability for base cases

TABLE II
BASE CASES - AVERAGE LS AND BLACKOUTS

	Case 1	Case 2	Case 3	Case 4	Case 5
Average LS	6.1 % ± 0.6	5.5 % ± 0.6	9.1% ± 0.9	6.8 % ± 0.7	4 % ± 0.4
Blackouts	1	18	55	29	10

2) Inertia Sensitivity analysis:

To evaluate the effect of the inertia on the resilience, the less resilient case of Section II-C is used as base case. Table III shows the different cases. They all have the same dispatch but different levels of inertia (obtained by increasing the inertia of the connected synchronous generators).

TABLE III
INERTIA SENSITIVITY ANALYSIS - CASES

	Base case	Case 2	Case 3	Case 4
System inertia	79.8 % I	95.8 % I	111.7 % I	127.7 % I
% of DERs generation	20	20	20	20

Figure 3 and Table IV show that the resilience is increasing in function of the level of inertia. This can be done in a more realistic way thanks to synthetic inertia.

In the next Section, the dynamic behaviour of the different cases of Section III-B1 for a specific scenario are analysed to highlights their difference.

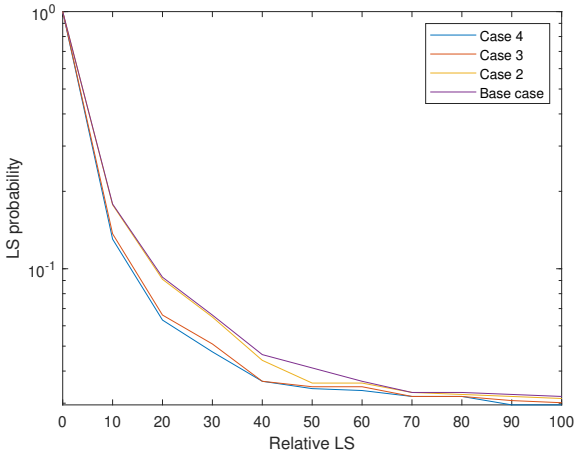

Fig. 3. LS probability for different inertia cases

TABLE IV
INERTIA STUDY CASES - AVERAGE LS AND BLACKOUTS

	Base case	Case 2	Case 3	Case 4
Average LS	9.1% ± 0.9	8.9 % ± 0.9	7.9 % ± 0.9	7.3 % ± 0.9
Blackouts	55	52	51	55

3) Specific scenario analysis:

The chosen scenario is the one that leads to the highest LS of Case 1 in section II-C as it is going against the statistical trend. Table V shows the different events that defined the scenario. The failure of the different lines results in sub-networks formation. In each sub-network frequency drop and possible lines overloading may occur. However as the dispatch and the inertia are different from one case to an other, the systems response may be different.

TABLE V
SCENARIO EVENTS

Failed transmission Lines	4-5	5-6	6-11	10-11	10-13	5-8	7-8	4-14	13-14
Time of failure (s)	1.3	1.3	1.5	1.7	2.1	3.8	3.8	5.7	6.1

Figure 4 shows the load power evolution for the 5 cases during the disaster.

For Case 1, the total power is provided by synchronous generators that are not located at the same nodes as the loads. The demand in some of the sub-networks is way higher that the generation. Thus, the minimum frequency reached is smaller than the minimum limit frequency which triggers the protections leading to LS. Other sub-networks have overloaded branches which leads to their opening and it results in the formation of smaller sub-networks. The ones

with high frequency drop will then be subject to LS.

The same type of response is observed for Case 2. However, as the dispatch is different, the LS does not occur at the same time and in the same sub-networks.

The worst case is Case 3. The failure of the different lines results in cascading events leading to a blackout.

Finally Case 4 and Case 5 seem to be very stable with almost no LS. The imbalance between the generation and the load in the different sub-networks does not lead to internal LS or overloaded branches and the important share of the generation is provided by the local production of DERs.

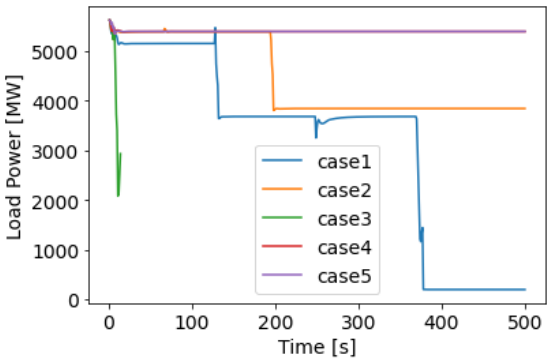

Fig. 4. Total load power evolution during and after the disaster

Figure 5 illustrates the frequency at node 1. It shows how the frequency variation is different from one case to an other as the power flows and the inertia are not the same. However, as there are different sub-networks for each case, the frequency may be different in other nodes.

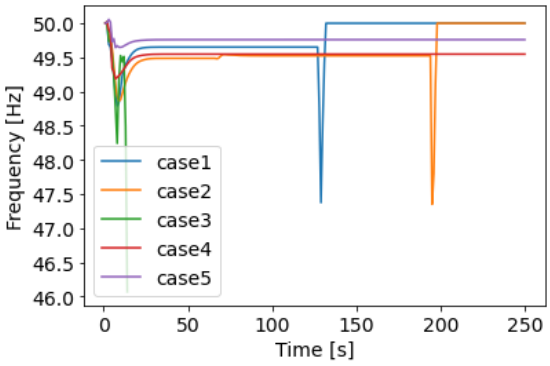

Fig. 5. Frequency evolution at node 1 during and after the disaster

IV. Conclusion

Using a combination of probabilistic assessment and dynamic simulations, this paper has show that integrating a significant proportion of DERs has complex effects on the resilience of the grid to natural disasters. Increasing the proportion DERs does not always enhance this resilience. In some scenarios, the effect of DERs is positive, while in others it is negative. How power is dispatched between synchronous generation and DERs, the structure of the grid, and which area of the power system is affected by the disaster all have an effect on the resilience and hence on the choice of and appropriate enhancement strategy. Further work will focus on modeling how DERs can supply local loads in the event of a blackout and how they can facilitate the restoration process.

References

[1] N. Bhual, M. Abdelmalak, M. Kamruzzaman, and M. Benidris, "Power system resilience: Current practices, challenges, and future directions," *IEEE Access*, no. 8, Jauary 2020.

[2] M. Panteli, D. N. Trakas, P. Mancarella, and N. D. Hatziargyriou, "Power systems resilience assessment: Hardening and smart operational enhancement strategies," in *Proceedings of the IEEE*, vol. 105, no. 7, 2017, pp. 1202–1213.

[3] N. Mahdavi Tabatabaei, S. Najafi Ravadanegh, and N. Bizon, *Power Sytems Resilience: Modeling, Analysis and Practice*. Springer, 2019.

[4] S. Espinoza, M. Panteli, P. Mancarella, and H. Rudnick, "Multi-phase assessment and adaptation of power systems resilience to natural hazards," *Electric Power Systems Research*, no. 136, March 2016.

[5] Y. Yang, W. Tang, Y. Liu, Y. Xin, and Q. Wu, "Quantitative resilience assessment for power transmission systems under typhoon weather," *IEEE Access*, no. 6, July 2018.

[6] F. Faghihi, P. Henneaux, P.-E. Labeau, and M. Panteli, "A probabilistic approach to dynamic resilience assessment of power systems," in *Proceedings of the 30th European Safety and Reliability Conference and 15th Probabilistic Safety Assessment and Management Conference (ESREL2020 PSAM15)*, November 2020.

[7] B. Johnson, V. Chalishazar, E. Cotilla-Sanchez, and T. K. Brekken, "A monte carlo methodology for earthquake impact analysis on the electrical grid," *Electric Power Systems Research*, vol. 184, p. 106332, 2020.

[8] T. Lagos, R. Moreno, A. N. Espinosa, M. Panteli, R. Sacaan, F. Ordonez, H. Rudnick, and P. Mancarella, "Identifying optimal portfolios of resilient network investments against natural hazards, with applications to earthquakes," *IEEE Transactions on Power Systems*, vol. 35, no. 2, pp. 1411–1421, 2020.

[9] M. Stubbe, A. Bihain, J. Deuse, and J. Baader, "Stag-a new unified software program for the study of the dynamic behaviour of electrical power systems," *IEEE Transactions on Power Systems*, vol. 4, no. 1, pp. 129–138, 1989.

[10] "Eurostag theory manuel," 1988-2018.

[11] G. Chaspierre, "Reduced-order modelling of active distribution networks for large-disturbance simulations," Ph.D. dissertation, Université de Liège, 2020.

[12] F. O. Resende, J. Matevosyan, and J. V. Milanovic, "Application of dynamic equivalence techniques to derive aggregated models of active distribution network cells and microgrids," in *2013 IEEE Grenoble Conference*, November 2013.

[13] A. V. Jayawardena., "Contributions to the development of microgrids: Aggregated modelling and operational aspects," Ph.D. dissertation, University of Wollongong, 2015.

[14] A. Morched, B. Gustavsen, and M. Tartibi, "A universal model for accurate calculation of electromagnetic transients on overhead lines and underground cables," *IEEE Transactions on Power Delivery*, no. 14, July 1999.

[15] F. Capitanescu, M. Glavic, D. Ernst, and L. Wehenkel, "Applications of security-constrained optimal power flows," in *Proceedings of Modern Electric Power Systems Symposium (MEPS06)*, 2006.

[16] P. Henneaux and D. S. Kirschen, "Probabilistic security analysis of optimal transmission switching," *IEEE Transactions on Power Systems*, vol. 31, no. 1, pp. 508–517, 2016.

[17] P. Demetriou, M. Asprou, J. Quiros-Tortos, and E. Kyriakides, "Dynamic ieee test systems for transient analysis," *IEEE Systems Journal*, vol. 11, no. 4, pp. 2108–2117, 2017.

[18] IEEE PES TF on Benchmarks for Validation of Emerging Power System Algorithms, "Power grid lib - optimal power flow." [Online]. Available: https://github.com/power-grid-lib/pglib-opf